

Thermal spin flips in atom chips

P.K. Rekdal,* S. Scheel, P.L. Knight, and E.A. Hinds

*Quantum Optics and Laser Science, Blackett Laboratory, Imperial College London,
Prince Consort Road, London SW7 2BW, United Kingdom*

(Dated: December 2, 2024)

We derive the spontaneous and thermal spin-flip rates for a neutral two-level ultra-cold atom that is coupled to a magnetic field. We apply this theory to an atom in the vicinity of a 2-layer cylindrical absorbing dielectric body surrounded by an unbounded homogeneous medium. An analytical expression is obtained for the spontaneous and thermal spin-flip rate in this particular geometry. The corresponding lifetime is then computed numerically. We compare these theoretical lifetimes to those measured by Jones et al. [M.P.A. Jones, C.J. Vale, D. Sahagun, B.V. Hall, and E.A. Hinds, Phys. Rev. Lett. **91**, 080401 (2003)]. We investigate how the lifetime depends on the materials (skin depths) of the cylindrical body. We also show how scaling of the dimensions of the cylindrical body affects the lifetime when (i) the distance from the wire to the atom is fixed and (ii) when the distance from the wire to the atom is scaled.

PACS numbers: 32.80.-t, 42.50.-p, 42.50.Ct

I. INTRODUCTION

Microscopic magnetic traps provide a powerful tool to control and manipulate the shape of Bose-Einstein condensates on a micrometer length scale. Microstructured surfaces, known as atom chips, are particularly interesting since they can be tailored to provide a variety of trapping geometries [1] and promise well-controlled quantum optical manipulations of neutral atoms in integrated and scalable microtrap arrays.

In these traps, atoms are strongly confined by electromagnetic fields close to nanostructured solid state substrates. Ultimately there is the possibility of controlling the quantum coherences within arrays of individual atoms for use in quantum information processing. This technology is attractive because it appears robust, scalable and because trapped neutral atoms can have long coherence times.

However, in metallic wires of finite conductivity at room temperature, thermal fluctuations give rise to Johnson noise currents [2]. These are normally observed as a noise voltage across a resistor, but they also cause the electromagnetic field near a conducting solid to fluctuate with a broad noise spectrum. For atoms trapped close to the surface of a conductor these fluctuating fields can be strong enough to drive rf magnetic dipole transitions that flip the atomic spin. If the atom is in a magnetic trap where only low-field-seeking Zeeman sublevels are confined, the spin-flips lead to atom loss. This is known experimentally [3, 4] as well as theoretically [5]. The loss rate increases strongly as the atoms approach the absorbing material, leading one to expect a limiting distance at which atoms can be stored above metallic surfaces.

The paper is organized as follows: In Section II we introduce the basic equations and discuss the quantization

of an electromagnetic field in the presence of a dispersing and absorbing dielectric body. Then, in Section III, we derive a general expression for the spontaneous and thermal spin-flip rates of a neutral two-level atom due to coupling of the atom's magnetic moment to a magnetic field. This derivation is based on the Zeeman Hamiltonian of the system and the corresponding Heisenberg equations of motion. We show that the spin-flip rate is determined by the imaginary part of the dyadic Green tensor of the classical, phenomenological Maxwell equations. In Section IV we present the scattering Green tensor for a 2-layer cylindrical body surrounded by an unbounded homogeneous medium. Then, in Section IV, we use this Green tensor to obtain an explicit analytical expression for the total spin-flip rate of an atom above a 2-layer cylindrical body at finite temperature and finite resistivity. Some numerical results are presented and discussed in Section VI. The numerical results are compared with the experimental measurements presented by Jones et al. in Ref. [3]. The scattering reflection coefficients corresponding to a 3-layer scattering Green tensor are given in the Appendix.

II. BASIC EQUATIONS AND QUANTIZATION

In classical electrodynamics, dielectric matter is commonly described in terms of a phenomenologically introduced dielectric susceptibility. Let us consider a classical electromagnetic field, described by the phenomenological Maxwell's equations, without external sources. We restrict our attention to isotropic but arbitrarily inhomogeneous non-magnetic media, and assume that the polarization responds linearly and locally to the electric field. A linear response formalism similar to that presented below can also be found in Refs. [6, 7].

The most general relation between the matter polarization and the electric field that is consistent with causality

*Electronic address: p.k.rekdal@imperial.ac.uk

and the fluctuation-dissipation theorem is [8]

$$\mathbf{P}(\mathbf{r}, t) = \varepsilon_0 \int_0^\infty d\tau [\varepsilon(\mathbf{r}, \tau) - 1] \mathbf{E}(\mathbf{r}, t - \tau) + \mathbf{P}_N(\mathbf{r}, t), \quad (1)$$

where $\varepsilon(\mathbf{r}, t)$ is the relative permittivity. The inclusion of the noise polarization $\mathbf{P}_N(\mathbf{r}, t)$ is necessary to fulfil the fluctuation-dissipation theorem. It is this fluctuating part of the polarization that is unavoidably connected with the loss in the medium. Converting the displacement field $\mathbf{D}(\mathbf{r}, t) = \varepsilon_0 \mathbf{E}(\mathbf{r}, t) + \mathbf{P}(\mathbf{r}, t)$ into Fourier space using Eq. (1), we obtain

$$\mathbf{D}(\mathbf{r}, \omega) = \varepsilon_0 \varepsilon(\mathbf{r}, \omega) \mathbf{E}(\mathbf{r}, \omega) + \mathbf{P}_N(\mathbf{r}, \omega), \quad (2)$$

where $\varepsilon(\mathbf{r}, \omega)$, being the temporal Fourier transform of $\varepsilon(\mathbf{r}, t)$, is the complex permittivity. The real part of the permittivity (ε_R responsible for the dispersion) and the imaginary part (ε_I responsible for absorption) are related to each other by the Kramers-Kronig relation.

Using Maxwell's equations in Fourier space, we find that $\mathbf{E}(\mathbf{r}, \omega)$ satisfies the Helmholtz equation

$$\nabla \times \nabla \times \mathbf{E}(\mathbf{r}, \omega) - \frac{\omega^2}{c^2} \varepsilon(\mathbf{r}, \omega) \mathbf{E}(\mathbf{r}, \omega) = \omega^2 \mu_0 \mathbf{P}_N(\mathbf{r}, \omega), \quad (3)$$

with the solution

$$\mathbf{E}(\mathbf{r}, \omega) = \omega^2 \mu_0 \int d^3 \mathbf{r}' \mathbf{G}(\mathbf{r}, \mathbf{r}', \omega) \cdot \mathbf{P}_N(\mathbf{r}', \omega), \quad (4)$$

where the Green tensor $\mathbf{G}(\mathbf{r}, \mathbf{r}', \omega)$, a second-rank tensor, is determined by the partial differential equation

$$\nabla \times \nabla \times \mathbf{G}(\mathbf{r}, \mathbf{r}', \omega) - \frac{\omega^2}{c^2} \varepsilon(\mathbf{r}, \omega) \mathbf{G}(\mathbf{r}, \mathbf{r}', \omega) = \delta(\mathbf{r} - \mathbf{r}'). \quad (5)$$

Together with the boundary condition at infinity, this equation has a unique solution. In accordance with Maxwell's equations the corresponding solution for the magnetic field in Fourier space is $\mathbf{B}(\mathbf{r}, \omega) = (i\omega)^{-1} \nabla \times \mathbf{E}(\mathbf{r}, \omega)$.

As we have seen, the noise polarization $\mathbf{P}_N(\mathbf{r}, t)$ plays a fundamental rôle in determining the electric field. Note, however, that its actual form follows from the fluctuation-dissipation theorem which states that the fluctuations of the macroscopic polarization are given by the imaginary part of the response function [here $\varepsilon(\mathbf{r}, \omega)$]. Thus, if we pull out a factor and define the dynamical variables $\mathbf{f}(\mathbf{r}, \omega)$ as the fundamental δ -correlated random process, we find that we can write the noise polarization as

$$\mathbf{P}_N(\mathbf{r}, \omega) = i \sqrt{\frac{\hbar \varepsilon_0}{\pi}} \varepsilon_I(\mathbf{r}, \omega) \mathbf{f}(\mathbf{r}, \omega). \quad (6)$$

Upon quantization, we replace the classical fields $\mathbf{f}(\mathbf{r}, \omega)$ by the operator-valued bosonic fields $\hat{\mathbf{f}}(\mathbf{r}, \omega)$ which we associate with the elementary excitations of the system composed of the electromagnetic field and the absorbing

dielectric matter. They satisfy the equal-time commutation relations $[\hat{f}_i(\mathbf{r}, \omega), \hat{f}_j^\dagger(\mathbf{r}', \omega')] = \delta_{ij} \delta(\mathbf{r} - \mathbf{r}') \delta(\omega - \omega')$.

The magnetic field operator in the Schrödinger picture can now be obtained as

$$\hat{\mathbf{B}}(\mathbf{r}) = \hat{\mathbf{B}}^{(+)}(\mathbf{r}) + \hat{\mathbf{B}}^{(-)}(\mathbf{r}), \quad \hat{\mathbf{B}}^{(+)}(\mathbf{r}) = [\hat{\mathbf{B}}^{(-)}(\mathbf{r})]^\dagger \quad (7)$$

where

$$\hat{\mathbf{B}}^{(-)}(\mathbf{r}) = \int_0^\infty d\omega \hat{\mathbf{B}}(\mathbf{r}, \omega), \quad (8)$$

is the negative-frequency part of the magnetic field operator. In this way, the electromagnetic field is expressed in terms of the classical Green tensor satisfying the Helmholtz equation (5) and the continuum of the fundamental bosonic field variables $\hat{\mathbf{f}}(\mathbf{r}, \omega)$. All the information about the dielectric matter is contained, via the permittivity $\varepsilon(\mathbf{r}, \omega)$, in the Green tensor of the classical problem.

We close this Section by mentioning two important properties of the Green tensor. It can be shown that the (Onsager) reciprocity relation $\mathbf{G}(\mathbf{r}, \mathbf{r}', \omega) = \mathbf{G}^T(\mathbf{r}', \mathbf{r}, \omega)$ holds [9]. Additionally, another useful property is the integral relation

$$\int d^3 \mathbf{r}' \frac{\omega^2}{c^2} \varepsilon_I(\mathbf{r}', \omega) G_{kl}(\mathbf{r}, \mathbf{r}', \omega) G_{nl}^*(\mathbf{r}_A, \mathbf{r}', \omega) = \text{Im } G_{kn}(\mathbf{r}, \mathbf{r}_A, \omega), \quad (9)$$

which we will use later in this paper. Both relations essentially follow from linear response theory, with Eq. (9) being equivalent to the fluctuation-dissipation theorem.

III. DERIVATION OF THE SPONTANEOUS AND THERMAL SPIN FLIP RATES

The Hamiltonian of the combined system of electromagnetic field and absorbing matter, from which the (quantized) phenomenological Maxwell's equations can be derived, can be written in terms of the basic field operators $\hat{\mathbf{f}}(\mathbf{r}, \omega)$ in the diagonal form

$$\hat{H} = \int d^3 \mathbf{r} \int_0^\infty d\omega \hbar \omega \hat{\mathbf{f}}^\dagger(\mathbf{r}, \omega) \cdot \hat{\mathbf{f}}(\mathbf{r}, \omega) + \sum_{\alpha=i,f} \hbar \omega_\alpha \hat{\xi}_\alpha, \quad (10)$$

which leads in the Heisenberg picture to the (quasi-free) time evolution $\hat{\mathbf{f}}(\mathbf{r}, \omega) \rightarrow \hat{\mathbf{f}}(\mathbf{r}, \omega) e^{-i\omega t}$. We have here introduced the dimensionless atomic operators $\hat{\xi}_\alpha \equiv |\alpha\rangle\langle\alpha|$, where $\hbar\omega_\alpha$ is the energy of the atomic state $|\alpha\rangle$ ($\alpha = i, f$).

The interaction of a neutral two-level atom at position \mathbf{r}_A with a magnetic field $\hat{\mathbf{B}}(\mathbf{r})$ is described by the Zeeman Hamiltonian $\hat{H}_Z = -\hat{\mu} \cdot \hat{\mathbf{B}}(\mathbf{r}_A)$, where $\hat{\mu} = \mu |i\rangle\langle f| + \text{h.c.}$ is the magnetic moment operator associated with the transition $|i\rangle \rightarrow |f\rangle$. The magnetic moment vector is

$$\mu = \langle i | \mu_B \left(g_S \hat{\mathbf{S}} + g_L \hat{\mathbf{L}} - g_I \frac{m_e}{m_p} \hat{\mathbf{I}} \right) | f \rangle, \quad (11)$$

where μ_B is the Bohr magneton, $\hat{\mathbf{S}}$ is the electronic spin operator, $\hat{\mathbf{L}}$ is the orbital angular momentum operator, $\hat{\mathbf{I}}$ is the nuclear spin operator and $g_S \approx 2$, g_L and g_I are the corresponding g -factors. We restrict our attention to $L = 0$, which corresponds to the ground state of an alkali atom, and we neglect the small nuclear magnetic moment in comparison with the Bohr magneton. In the rotating-wave approximation, we can then write the Zeeman Hamiltonian as

$$\hat{H}_Z \approx -\mu_B g_S \left[\langle f | \hat{S}_q | i \rangle \hat{\xi}^{(+)} \hat{B}_q^{(+)}(\mathbf{r}_A) + \text{h.c.} \right], \quad (12)$$

where the dimensionless atomic raising (lowering) operator $\hat{\xi}^{(+)} \equiv |i\rangle\langle f|$ ($\hat{\xi}^{(-)} = (\hat{\xi}^{(+)})^\dagger$) satisfy the commutation relation $[\hat{\xi}_z, \hat{\xi}^{(\pm)}] = \pm \hat{\xi}^{(\pm)}$, with $\hat{\xi}_z \equiv \frac{1}{2}(|f\rangle\langle f| - |i\rangle\langle i|)$. Repeated indices q indicate a sum over spatial vector components.

Using the Hamiltonian (12), the Heisenberg equation of motion for the atomic quantity $\hat{\xi}_z(t)$ is given by

$$\dot{\hat{\xi}}_z(t) = -\frac{\mu_B g_S}{i\hbar} \langle f | \hat{S}_q | i \rangle \hat{\xi}^{(+)} \hat{B}_q^{(+)}(\mathbf{r}_A) + \text{h.c.} \quad (13)$$

Furthermore, the Heisenberg equation of motion for the bosonic field operator is

$$\begin{aligned} \dot{\hat{f}}_i(\mathbf{r}, \omega, t) &= -i\omega \hat{f}_i(\mathbf{r}, \omega, t) \\ &+ \frac{i\mu_B g_S}{\sqrt{\hbar\pi\varepsilon_0}} \langle f | \hat{S}_q | i \rangle \hat{\xi}^{(-)} \epsilon_{qpj} \partial_p \frac{\omega}{c^2} \sqrt{\varepsilon_I(\mathbf{r}, \omega)} G_{ji}^*(\mathbf{r}_A, \mathbf{r}, \omega), \end{aligned} \quad (14)$$

where ϵ_{qpj} is the Levi-Civita symbol and $\partial_j \equiv \partial/\partial x_j$. This equation can now be formally integrated to yield

$$\begin{aligned} \hat{f}_i(\mathbf{r}, \omega, t) &= \hat{f}_{i,\text{free}}(\mathbf{r}, \omega, t) + \int_{t'}^t d\tau e^{-i\omega(t-\tau)} \hat{\xi}^{(-)}(\tau) \\ &\times \frac{i\mu_B g_S}{\sqrt{\hbar\pi\varepsilon_0}} \langle f | \hat{S}_q | i \rangle \epsilon_{qpj} \partial_p \frac{\omega}{c^2} \sqrt{\varepsilon_I(\mathbf{r}, \omega)} G_{ji}^*(\mathbf{r}_A, \mathbf{r}, \omega), \end{aligned} \quad (15)$$

where $\hat{f}_{i,\text{free}}(\mathbf{r}, \omega, t)$ denotes the freely evolving basic-field operators. The lowering operator $\hat{\xi}^{(-)}(\tau)$ in Eq. (15) can be found by solving its Heisenberg equation of motion. In the Markov approximation, this solution can be reduced to its slowly varying part $\hat{\xi}^{(-)}(t) e^{i\omega_{fi}(t-\tau)}$ in Eq. (15) so that the time integral can be approximated by

$$\begin{aligned} \hat{f}_i(\mathbf{r}, \omega, t) &= \hat{f}_{i,\text{free}}(\mathbf{r}, \omega, t) + \frac{i\mu_B g_S}{\sqrt{\hbar\pi\varepsilon_0}} \langle f | \hat{S}_q | i \rangle \hat{\xi}^{(-)}(t) \\ &\times \epsilon_{qpj} \partial_p \frac{\omega}{c^2} \sqrt{\varepsilon_I(\mathbf{r}, \omega)} G_{ji}^*(\mathbf{r}_A, \mathbf{r}, \omega) \zeta(\omega_{fi} - \omega), \end{aligned} \quad (16)$$

where $\zeta(x) = \pi\delta(x) + i\mathcal{P}x^{-1}$ (\mathcal{P} denotes the principal value) and $\omega_{fi} \equiv \omega_f - \omega_i$ is the transition frequency corresponding to the flip $|i\rangle \rightarrow |f\rangle$ in the atom's internal state. Substituting this formal solution into the expression for the magnetic field, we obtain

$$\begin{aligned} \hat{B}_q^{(+)}(\mathbf{r}_A, \omega, t) &= \hat{B}_{q,\text{free}}^{(+)}(\mathbf{r}_A, \omega, t) \\ &+ i\mu_B g_S \mu_0 \langle f | \hat{S}_p | i \rangle \epsilon_{qjk} \epsilon_{pmn} \partial_j \partial_m \hat{\xi}^{(-)}(t) \zeta(\omega_{fi} - \omega) \\ &\times \int d^3\mathbf{r} \frac{\omega^2}{c^2} \varepsilon_I(\mathbf{r}, \omega) G_{kl}(\mathbf{r}_A, \mathbf{r}, \omega) G_{nl}^*(\mathbf{r}_A, \mathbf{r}, \omega). \end{aligned} \quad (17)$$

The spatial integral can be evaluated using the integral relation Eq. (9) yielding $\text{Im} G_{kn}(\mathbf{r}_A, \mathbf{r}_A, \omega)$. Therefore, Eq. (17) becomes

$$\begin{aligned} \hat{B}_q^{(+)}(\mathbf{r}_A, \omega, t) &= \hat{B}_{q,\text{free}}^{(+)}(\mathbf{r}_A, \omega, t) \\ &+ i\mu_B g_S \mu_0 \langle f | \hat{S}_k | i \rangle \hat{\xi}^{(-)}(t) \zeta(\omega_{fi} - \omega) \\ &\times \text{Im} [\nabla \times \nabla \times \mathbf{G}(\mathbf{r}_A, \mathbf{r}_A, \omega)]_{qk}. \end{aligned} \quad (18)$$

Performing the ω -integration and inserting into Eq. (13), we obtain

$$\begin{aligned} \dot{\hat{\xi}}_z(t) &= -(\Gamma^B + i\delta\omega) [\frac{1}{2} + \hat{\xi}_z(t)] \\ &+ \left[\frac{\mu_B g_S}{\hbar^2} \langle f | \hat{S}_q | i \rangle \hat{\xi}^{(+)} \hat{B}_{q,\text{free}}^{(+)}(\mathbf{r}_A) + \text{h.c.} \right], \end{aligned} \quad (19)$$

where the spontaneous spin-flip rate $\Gamma^B \equiv \Gamma^B(\mathbf{r}_A, \tilde{\omega}_{fi})$ arises from the δ function (the real part of the ζ function) and is given by

$$\begin{aligned} \Gamma^B &= \mu_0 \frac{2(\mu_B g_S)^2}{\hbar} \langle f | \hat{S}_q | i \rangle \langle i | \hat{S}_p | f \rangle \\ &\times \text{Im} [\nabla \times \nabla \times \mathbf{G}(\mathbf{r}_A, \mathbf{r}_A, \tilde{\omega}_{fi})]_{qp}, \end{aligned} \quad (20)$$

and where the term $\delta\omega$ arises from the principal-value integral (the imaginary part of the ζ function) and is identified as the radiative frequency shift. Furthermore, the shifted frequency is given by $\tilde{\omega}_{fi} = \omega_{fi} + \delta\omega$. In what follows, the transition frequency is always taken to be the shifted frequency $\tilde{\omega}_{fi}$ that one measures in an experiment instead of the bare frequency $\omega_{fi} \equiv \omega$. For simplicity, we omit the tilde in all subsequent formulas. Note that the same result for Γ^B is obtained when using an appropriately derived master equation as done in Ref. [5].

We assume that the dielectric body is in thermal equilibrium with the surroundings. The magnetic field is then in a thermal state with a temperature T , equal to the temperature of the dielectric body. The total flip rate for the atom is therefore given by $\Gamma_{\text{total}}^B = \Gamma^B(\bar{n}_{\text{th}} + 1)$, where the mean thermal occupation number is

$$\bar{n}_{\text{th}} = \frac{1}{e^{\hbar\omega_{fi}/k_B T} - 1}, \quad (21)$$

and k_B is Boltzmann's constant. At zero temperature, i.e. $\bar{n}_{\text{th}} = 0$, the relaxation dynamics is entirely due to spontaneous flip rate Γ^B . Heating processes are suppressed. For large T on the other hand, i.e. $\hbar\omega_{fi}/k_B T \ll 1$, we have $\bar{n}_{\text{th}} \approx \frac{k_B T}{\hbar\omega_{fi}} \gg 1$. The relaxation dynamics is in this case dominated by flip rate induced by thermal fluctuations.

In the experiment of Ref. [3] ^{87}Rb atoms are initially pumped into the trapped state $|F, m\rangle = |2, 2\rangle$. Thermal fluctuations of the magnetic field may then cause the atoms to evolve into hyperfine sublevels with lower m_F . Atoms evolving into the state with $m_F = 1$ are still trapped. Atoms with $m_F = 0$, however, fall out of the trap under gravity as they experience no trapping

force and atoms with $m_F < 0$ are rapidly expelled by the magnetic forces. We can therefore assume that the probability for the atoms to be thermally pumped back into a trapped state is negligible. If, in addition, we assume that the rate-limiting transition is $|2, 2\rangle \rightarrow |2, 1\rangle$, then the lifetime for the atoms to remain in the trap is determined by the inverse of the spin-flip rate Γ_{21}^B , where we have introduced the notation $\Gamma_{m_i m_f}^B$ for the total spin-flip rate associated with the transition $|2, m_i\rangle \rightarrow |2, m_f\rangle$.

On the other hand, there might be a non-negligible probability for the atoms with $m_F = 0$ to be thermally pumped back into a trapped state (but atoms with $m_F < 0$ are still rapidly expelled from the trap). Let us in this case assume that each transition between two neighbouring levels occur at the same frequency. We can then write $\Gamma_{10}^B = 3/2 \Gamma_{21}^B$. For large T , i.e. $\bar{n}_{\text{th}} \gg 1$, we can also put $\Gamma_{12}^B = \Gamma_{21}^B$. The occupation number $n_{m_F}(t)$ for the state $|2, m_F\rangle$ is then

$$\frac{n_2(t)}{n_2(0)} = \frac{1}{5} e^{-3\Gamma_{21}^B t} + \frac{4}{5} e^{-\frac{1}{2}\Gamma_{21}^B t}, \quad (22)$$

$$\frac{n_1(t)}{n_2(0)} = -\frac{2}{5} e^{-3\Gamma_{21}^B t} + \frac{2}{5} e^{-\frac{1}{2}\Gamma_{21}^B t}, \quad (23)$$

and $n_2(t)/n_2(0) = 1 - n_1(t)/n_2(0) - n_2(t)/n_2(0)$. The long-time behaviour of the occupation number $n_{m_F}(t)$ is therefore determined by the last exponential term in the above equations, in which case the total spin-flip rate is half of the rate Γ_{21}^B .

IV. THE DYADIC GREEN TENSOR

The geometry we are considering in this paper is a 2-layer cylinder surrounded by an unbounded homogeneous medium (see Fig. 1). This corresponds to the experimental geometry in Ref. [3]. Because the Helmholtz equation is linear, the associated Green tensor can be written as a sum according to

$$\mathbf{G}(\mathbf{r}, \mathbf{r}', \omega) = \mathbf{G}^0(\mathbf{r}, \mathbf{r}', \omega) + \mathbf{G}^{\text{wire}}(\mathbf{r}, \mathbf{r}', \omega), \quad (24)$$

where $\mathbf{G}^0(\mathbf{r}, \mathbf{r}', \omega)$ represents the contribution of the direct waves from the radiation sources in an unbounded medium, which is vacuum in our case, and $\mathbf{G}^{\text{wire}}(\mathbf{r}, \mathbf{r}', \omega)$ describes the scattering contribution of multiple reflection waves from the wire. When the atom is located in the outermost layer, the scattering contribution is [10]

$$\mathbf{G}^{\text{wire}}(\mathbf{r}, \mathbf{r}', \omega) = \frac{i}{8\pi} \int_{-\infty}^{\infty} dh \sum_{n=0}^{\infty} \frac{2 - \delta_{0n}}{\eta_3^2} \mathcal{R}_n(h) \quad (25)$$

where

$$\mathcal{R}_n(h) = R_n^{11}(h) \left[\mathbf{N}_{e_n}^{(1)}(h) \mathbf{N}_{e_n}^{(1)}(-h) + \mathbf{N}_{o_n}^{(1)}(h) \mathbf{N}_{o_n}^{(1)}(-h) \right]$$

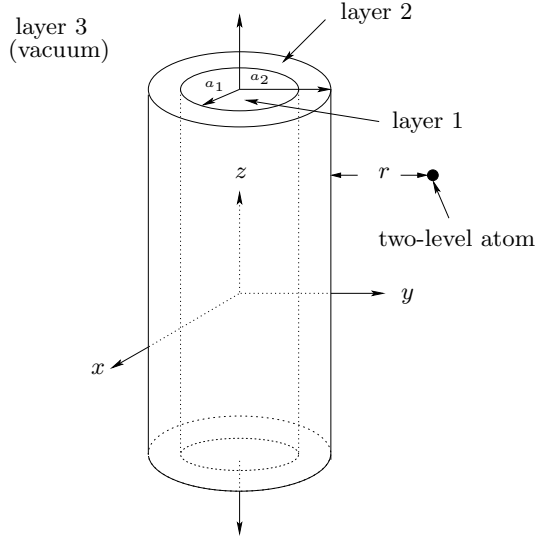


FIG. 1: The geometry we are considering is a 2-layer cylinder surrounded by an unbounded homogeneous medium, i.e. in total a 3-layer cylindrical geometry. The outermost layer is labelled layer 3 (vacuum), the coating layer is layer 2 and the cylinder core is layer 1. Note that r is the distance from the surface of the outermost layer to the atom.

$$\begin{aligned} &+ R_n^{12}(h) \left(-\frac{\omega \varepsilon_3}{k_3} \right) \quad (26) \\ &\times \left[\mathbf{N}_{e_n}^{(1)}(h) \mathbf{M}_{o_n}^{(1)}(-h) - \mathbf{N}_{o_n}^{(1)}(h) \mathbf{M}_{e_n}^{(1)}(-h) \right. \\ &\quad \left. + \mathbf{M}_{e_n}^{(1)}(h) \mathbf{N}_{o_n}^{(1)}(-h) - \mathbf{M}_{o_n}^{(1)}(h) \mathbf{N}_{e_n}^{(1)}(-h) \right] \\ &+ R_n^{22}(h) \left[\mathbf{M}_{e_n}^{(1)}(h) \mathbf{M}_{e_n}^{(1)}(-h) + \mathbf{M}_{o_n}^{(1)}(h) \mathbf{M}_{o_n}^{(1)}(-h) \right]. \end{aligned}$$

For simplicity, we have omitted the tensor product symbol \otimes between the even and odd cylindrical vector wave functions defined by $\mathbf{M}_{e_n}^{(1)}(h) = \nabla \times [\psi_{e_n}^{(1)}(h) \mathbf{z}]$ and $\mathbf{N}_{e_n}^{(1)}(h) = \nabla \times \nabla \times [\psi_{e_n}^{(1)}(h) \mathbf{z}] / k_3$. The scalar eigenfunctions $\psi_{e_n}^{(1)}(h)$ satisfy the homogeneous scalar wave equation [10]. From these definitions we immediately realize that the vector wave functions are related by

$$\nabla \times \mathbf{M}_{e_n}^{(1)}(h) = k_3 \mathbf{N}_{e_n}^{(1)}(h), \quad (27)$$

$$\nabla \times \mathbf{N}_{e_n}^{(1)}(h) = k_3 \mathbf{M}_{e_n}^{(1)}(h). \quad (28)$$

Written out explicitly, they are given by

$$\begin{aligned} \mathbf{N}_{e_n}^{(1)}(h) &= \frac{1}{k_3} \left[i h \frac{dZ_n(\eta_3 \rho)}{d\rho} \frac{\cos(n\phi)}{\sin(n\phi)} \mathbf{e}_\rho \right. \\ &\quad \left. \mp i h \frac{n}{\rho} Z_n(\eta_3 \rho) \frac{\sin(n\phi)}{\cos(n\phi)} \mathbf{e}_\phi + \eta_3^2 Z_n(\eta_3 \rho) \frac{\cos(n\phi)}{\sin(n\phi)} \mathbf{e}_z \right] e^{ihz}, \end{aligned} \quad (29)$$

$$\begin{aligned} \mathbf{M}_{e_n}^{(1)}(h) &= \left[\mp \frac{n}{\rho} Z_n(\eta_3 \rho) \frac{\sin(n\phi)}{\cos(n\phi)} \mathbf{e}_\rho \right. \\ &\quad \left. - \frac{dZ_n(\eta_3 \rho)}{d\rho} \frac{\cos(n\phi)}{\sin(n\phi)} \mathbf{e}_\phi \right] e^{ihz}. \end{aligned} \quad (30)$$

The primes in Eq. (26) indicate the spherical coordinates (ρ', ϕ', z') . The superscript (1) indicates that Z_n should be replaced by the Hankel function of first kind $H_n^{(1)}$. Otherwise, Z_n is the Bessel function of first kind J_n . The propagation constant in the ρ direction is $\eta_p^2 = k_p^2 - h^2$, where k_p is the wave number of the p th layer. The permittivity of the p th layer is denoted by ε_p . The scattering reflection coefficients $R_n^{kl}(h)$ are given in Appendix A ($k, l = 1, 2$).

The double curl of the Green tensor in Eq. (25) can be written

$$\nabla \times \nabla' \times \mathbf{G}^{\text{wire}}(\mathbf{r}, \mathbf{r}', \omega) = \frac{i}{8\pi} \sum_{n=0}^{\infty} (2 - \delta_{0n}) \begin{bmatrix} (I_n)_{xx} & (I_n)_{xy} & (I_n)_{xz} \\ (I_n)_{yx} & (I_n)_{yy} & (I_n)_{yz} \\ (I_n)_{zx} & (I_n)_{zy} & (I_n)_{zz} \end{bmatrix}, \quad (31)$$

where

$$\mathbf{I}_n \equiv \mathbf{I}_n(\mathbf{r}, \mathbf{r}', \omega) = \int_{-\infty}^{\infty} dh \frac{1}{\eta_3^2} \nabla \times \nabla' \times \mathcal{R}_n(h). \quad (32)$$

Note that the curls are computed by replacing $\mathbf{N}_{\circ n}(h)$ by $\mathbf{M}_{\circ n}(h)$ and vice versa, according to Eqs. (27) and (28). Also note that the integration variable h is the wave number in the z -direction (see Fig. 1). Due to symmetry of the integrand, it is easy to show that $(I_n^{\text{lim}})_{xz} = (I_n^{\text{lim}})_{zx} = (I_n^{\text{lim}})_{yz} = (I_n^{\text{lim}})_{zy} = 0$, where $(I_n^{\text{lim}})_{ij} \equiv \lim_{\mathbf{r} \rightarrow \mathbf{r}'} (I_n(\mathbf{r}, \mathbf{r}', \omega))_{ij}$ ($i, j = x, y, z$). Note that the (Onsager) reciprocity relation as mentioned in Section II implies that $(I_n^{\text{lim}})_{ij} = (I_n^{\text{lim}})_{ji}$.

V. THE SPIN FLIP RATE FOR A 3-LAYER CYLINDRICAL GEOMETRY

The spin-flip rate in free space is readily derived from Eq. (20) since $\text{Im}[\nabla \times \nabla \times \mathbf{G}(\mathbf{r}_A, \mathbf{r}_A, \omega_{if})]_{qp} = (k_3^3/6\pi) \delta_{qp}$, where $k_3 = \omega/c$ is the free space wave number corresponding to the atomic transition. We use the notation k_3 here because in our discussion of the cylindrical wire, the third layer is also a vacuum. We obtain

$$\Gamma_{if}^0 = \mu_0 \frac{(\mu_B g_S)^2}{3\pi \hbar} k_3^3 S_{if}^2, \quad (33)$$

where we have introduced the angular factor $S_{if}^2 \equiv |\langle i | \hat{S}_x | f \rangle|^2 + |\langle i | \hat{S}_y | f \rangle|^2 = 2 |\langle i | \hat{S}_x | f \rangle|^2$. We do not have any term containing the matrix element of \hat{S}_z since we are interested here in a spin-flip Hamiltonian, which by definition changes m_F . We have furthermore used that the absolute value two matrix elements are equal as a result of symmetry.

In order to find the contribution of the wire to the spontaneous spin-flip rate, we use Eqs. (20) and (31), which gives

$$\Gamma_{if}^{\text{wire}} = \frac{3}{8} \Gamma_{if}^0 \sum_{n=0}^{\infty} (2 - \delta_{0n}) \text{Re} \left[(\tilde{I}_n^{\text{lim}})_{xx} + (\tilde{I}_n^{\text{lim}})_{yy} \right], \quad (34)$$

where we once again have used the fact that $|\langle i | \hat{S}_x | f \rangle|^2 = |\langle i | \hat{S}_y | f \rangle|^2$ as well as $\langle i | \hat{S}_z | f \rangle = 0$, and where the dimensionless integrals $(\tilde{I}_n^{\text{lim}})_{ij} \equiv (I_n^{\text{lim}})_{ij}/k_3^3$ are given by

$$\begin{aligned} (\tilde{I}_n^{\text{lim}})_{xx} + (\tilde{I}_n^{\text{lim}})_{yy} &= \int_{-\infty}^{\infty} dq \frac{1}{\tilde{\eta}_3^2} \times \\ &\left\{ [R_n^{11}(q) + q^2 R_n^{22}(q)] [(H_{n3})^2 \frac{n^2}{k_3^2(a_2 + r)^2} + (\tilde{\eta}_3 H'_{n3})^2] \right. \\ &\left. + 2iqR_n^{12}(q) \left(-\frac{\omega \varepsilon_3}{k_3} \right) \tilde{\eta}_3 (H_{n3}^2)' \frac{n}{k_3(a_2 + r)} \right\}, \end{aligned} \quad (35)$$

since $\rho = a_2 + r$. Note that $(\tilde{I}_n^{\text{lim}})_{xy}$ and $(\tilde{I}_n^{\text{lim}})_{yx}$ do not appear in Eq. (35). In these expressions, we have chosen (for convenience) to write the permittivity of the p th layer relative to the outermost layer, i.e. $\varepsilon_p = \varepsilon_3 \varepsilon_p^{\text{rel}}$. The wave number for layer p is therefore given by $k_p^2 = k_3^2 \varepsilon_p^{\text{rel}}$. The relative permittivity is dimensionless and in general complex. The dimensionless propagation constant $\tilde{\eta}_p \equiv \eta_p/k_3$ in ρ direction can in this case be written $\tilde{\eta}_p = \sqrt{\varepsilon_p^{\text{rel}} - q^2}$, where the dimensionless integration variable is $q \equiv h/k_3$. We have here used the simplified notation $Z_{np} \equiv Z_n(\tilde{\eta}_p k_3 \rho)$. Furthermore, the primes in Eq. (35) denote the derivate with respect to the full argument of the relevant function, e.g. $Z'_{np} \equiv dZ_n(\tilde{\eta}_p k_3 \rho)/d(\tilde{\eta}_p k_3 \rho)$.

The skin depth is the characteristic length scale on which an electromagnetic wave is damped within a conducting medium. It is given by $\delta_p = \sqrt{2\varepsilon_0 \rho_p \omega}/k_0$ (see e.g. Ref. [11]), where ρ_p is the resistivity of layer p . Since our atomic transition frequency is much smaller than the resonance frequency of the dielectric(s) in the wire, the relative permittivity is related to the skin depth by [11]

$$\varepsilon_p^{\text{rel}} \approx \frac{i}{\varepsilon_0 \rho_p \omega} = i \frac{2}{k_0^2 \delta_p^2}, \quad (36)$$

corresponding to absorption only since it is purely imaginary.

Due to Eq. (24), the total spin-flip rate is equal to the sum of the free space contribution and the scattering contribution. The total spin-flip rate for the rate-limiting transition $|2, 2\rangle \rightarrow |2, 1\rangle$ is then

$$\Gamma_{21}^B = (\Gamma_{21}^0 + \Gamma_{21}^{\text{wire}}) (\bar{n}_{\text{th}} + 1), \quad (37)$$

where both spin-flip rate on the right-hand-side contains an angular factor $S_{21}^2 = 1/8$ [15]. The lifetime τ for the atom to remain in the trap is the inverse of Eq. (37).

VI. NUMERICAL RESULTS

In a recent paper by Jones et al. [3] an experiment is described in which cold atoms are held in a microscopic trap at room-temperature near a current-carrying wire. The lifetime for atoms to remain in the microtrap is measured over a range of distances down to $27 \mu\text{m}$ from the

surface of the wire. The wire consists of a central copper (Cu) core with radius $a_1 = 185 \mu\text{m}$ and a $55 \mu\text{m}$ thick aluminium (Al) layer, i.e. $a_2 = 240 \mu\text{m}$. The resistivities for Cu and Al are $\rho_1 = 1.6 \cdot 10^{-8} \Omega\text{m}$ and $\rho_2 = 2.7 \cdot 10^{-8} \Omega\text{m}$, respectively. Together with Eq. (36), this corresponds to the skin depths $\delta_1 = 85 \mu\text{m}$ and $\delta_2 = 110 \mu\text{m}$, at the frequency $f = \omega/2\pi = 560 \text{ kHz}$.

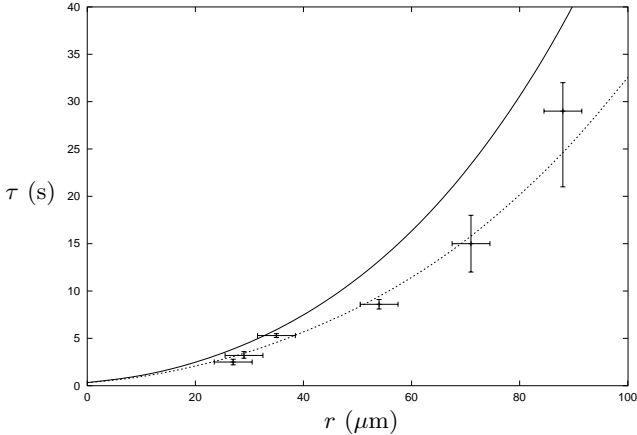


FIG. 2: Lifetime τ of the trapped atom as a function of the atom-surface distance r . *Solid curve*: calculated lifetime for a 3-layer cylindrical geometry with the parameters $a_1 = 185 \mu\text{m}$, $a_2 = 240 \mu\text{m}$, $\delta_1 = 85 \mu\text{m}$, and $\delta_2 = 110 \mu\text{m}$. *Dotted curve*: calculated lifetime for a thick Al slab with $\delta = 110 \mu\text{m}$ (using Eq. (35) in Ref. [5]). *Crosses*: experimental measurements in Ref. [3]. The other parameters are: $f = 560 \text{ kHz}$ and $T = 300 \text{ K}$, for all graphs.

The calculated result (solid curve) as well as the experimental measurements (crosses) are shown in Fig. 2. We observe that the theoretical calculation predicts longer lifetimes than actually measured in [3]. For the r -range under consideration, theory and experiment differ by a factor of approximately 1.4. This is a rather small discrepancy showing that the trapping losses are indeed predominantly caused by thermal spin-flips.

The theory for the decay rate of an atom above a plane, thick slab is also known [5]. Applying this theory to an Al slab with skin depth $\delta = 110 \mu\text{m}$, we obtain the result as shown in the dotted curve in Fig. 2. We observe that the lifetime of an atom above the slab is shorter than the corresponding lifetime of an atom above the wire. This is what one would expect since the slab contains more spin-flip inducing material than the wire. We furthermore observe that four of the measured lifetimes are even shorter than the corresponding lifetimes of an atom above the slab.

For sufficiently small atom-surface distances ($r \ll \delta_2, \delta_1, a_2$) the spin-flip lifetime of an atom above the slab coincide with that of an atom above the cylindrical wire (see Fig. 2). This is as one would expect since the electromagnetic field very close to such a wire behaves as if it is induced by a plane slab. According to Ref. [5], the spin-flip lifetime of an atom above of a slab is linear in the atom-surface distance provided that $z \ll \delta$ (z is the

distance from the surface of the slab to the atom). For $r \lesssim 20 \mu\text{m}$ the lifetime of an atom above the wire is also linear with the atom-surface distance for the parameters under consideration in Fig. 2.

The lifetime for the atom to remain in the trap depends strongly on the skin depth of the material(s). This fact is illustrated in Fig. (3), where the skin depth of the wire core δ_1 is fixed at $85 \mu\text{m}$ but the skin depth of the outer layer δ_2 is varied. For a given δ_2 , there are two competing effects: As the skin depth decreases, the amount of radiation per unit volume grows [see Eqs. (6) and (36)] but the volume of the dielectric body that causes radiation decreases. When the “volume-decrease” is stronger than the “radiation-increase” the lifetime of the trapped atom increases with decreasing skin depth. This is the case for $\delta_2 \lesssim 20 \mu\text{m}$ in Fig. 3. In the small δ_2 limit the outer layer approaches a perfect conductor, i.e. the core wire does not play any role in this limit. On the other hand, for $\delta_2 \gtrsim 20 \mu\text{m}$ in Fig. 3, it is the other way around: The lifetime is growing with increasing skin depth. This means that a worse conductor gives longer lifetime. In the large δ_2 -limit the outer layer of the wire approaches the free space limit, and the lifetime is entirely determined by the skin depth and the radius of the core of the wire. The numerical value for this limit is 51.7 s for the parameters under consideration in Fig. 3.

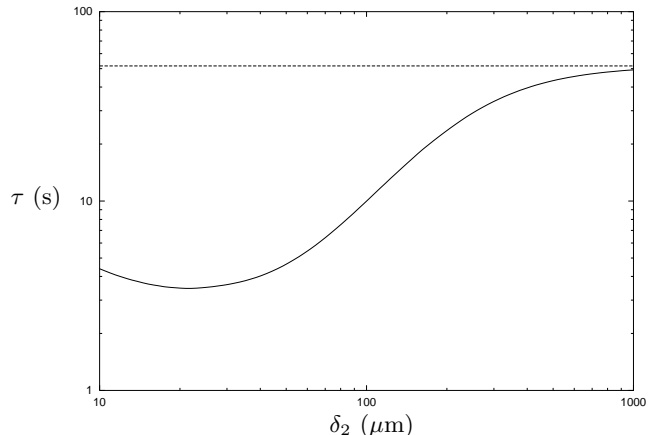


FIG. 3: Lifetime τ of the trapped atom as a function of the skin depth δ_2 of the outer layer. The atom-surface distance is fixed at $r = 50 \mu\text{m}$. The other parameters are: $f = 560 \text{ kHz}$, $T = 300 \text{ K}$, $a_1 = 185 \mu\text{m}$, $a_2 = 240 \mu\text{m}$, and $\delta_1 = 85 \mu\text{m}$. The straight dashed line represents the large δ_2 limit. The numerical value for this limit is 51.7 s for the parameters under consideration.

One of the goals in atom optics is to control cold atoms trapped above small integrated circuits, known as atom chips. It is therefore interesting to see how the lifetime is affected when the dimensions of the wire as well as the atom-surface distance are varied. While varying r , we scale the dimensions of the wire according to $a_2 = 5r$ and $a_1 = (185/240)a_2$. The skin depths, however, are fixed. The effects of such a scaling are illustrated in Fig. 4. For large atom-surface distance and large size

wires, i.e. $r \propto a_2 \gg \delta_2 \sim 100\mu\text{m}$, the spin-flip lifetime scales as $\sim r^4$. According to Ref. [5], the lifetime of an atom above a slab scales as z^4 as well (z is the distance from the surface of the slab to the atom) provided that $z \gg \delta$. It might therefore seem like the curvature of the wire becomes less significant for large size wires and large distances r , even though the ratio of the wire size and the atom-surface distance is fixed ($a_2/r = 5$). Hence, the electromagnetic field behaves in this case as if it is induced by a plane slab. By contrast, the small r limit is more complex. In this limit the atom gets infinitely close to an infinitely small wire. One can show that the term $\Gamma_{if}^{\text{wire}}$ scales as $1/r^2$ in the small $r \propto a_2$ -limit, i.e. the flip rate due to the wire gives a divergent contribution. There might be several possible explanations for this behaviour: As the dimensions of the wire are scaled down to a microscopic level, the permittivity as given by Eq. (36) does not give a correct description of the absorbing dielectric media since it is a macroscopic quantity. Furthermore, the Green tensor formalism breaks down in this limit since the surface boundary conditions are not well defined. We do not know, however, at what length scale this breakdown occurs. Most likely it happens far below the micrometer length scale we are considering in this paper. It is also hard to imagine a wire with radius of the order a few atomic lengths and at the same time carrying a current of several Ampere. If we

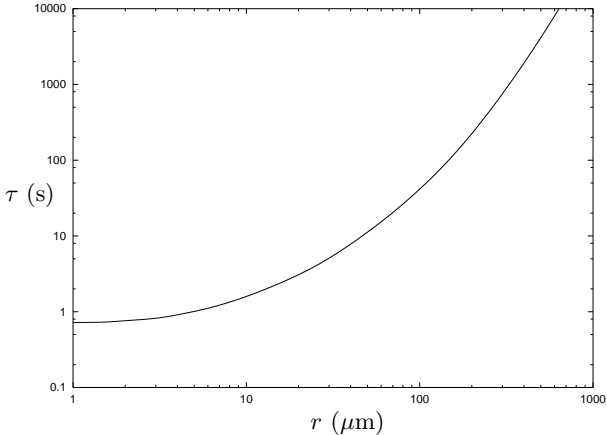


FIG. 4: The lifetime τ as a function of the atom-surface distance r . The dimensions of wire is scaled according to $a_2 = 5r$ and $a_1 = (185/240)a_2$. The other parameters are: $f = 560$ kHz, $T = 300$ K, $\delta_1 = 85\mu\text{m}$, and $\delta_2 = 110\mu\text{m}$.

fix the distance r but scale the dimensions of the wire according to $a_1 = (185/240)a_2$, keeping the skin depths fixed, then we obtain the result as shown in Fig. 5. The lifetime increases rapidly as the size of the wire is scaled down: when the dimensions of the wire are smaller than the skin depths, i.e. $a_2 \ll \delta_1, \delta_2$ ($\sim 100\mu\text{m}$ as in Fig. 5), the lifetime scales as a_2^{-3} . In the absence of a wire, i.e. $a_2 = 0$ but r fixed, we have $\Gamma_{if}^{\text{wire}} = 0$. The lifetime for the atoms to remain in the trap is then determined by the blackbody radiation only. For $f = 560$ kHz and $T = 300$ K, the numerical value for this free space lifetime is as

tonishing $\sim 10^{18}$ s [c.f. Eq. (37)]. Furthermore, in the large a_2 -limit (with r still fixed) the wire has no curvature. In this limit the lifetime of the atom approaches a constant value, being the lifetime of an atom above a slab with $\delta = \delta_2$. For the parameters under consideration, this lifetime is 8.2 s (see dotted curve in Fig. 5).

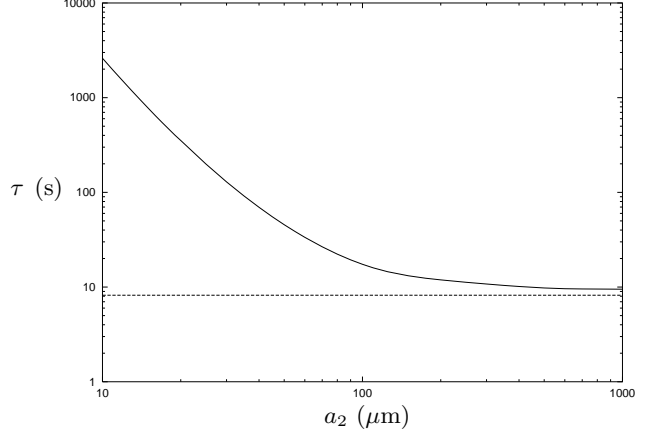


FIG. 5: The lifetime τ as a function of the outer wire radius a_2 . The atom-surface distance is fixed at $r = 50\mu\text{m}$. The dimensions of the wire is scaled according to $a_1 = (185/240)a_2$. The other parameters are: $f = 560$ kHz, $T = 300$ K, $\delta_1 = 85\mu\text{m}$, and $\delta_2 = 110\mu\text{m}$. The straight dashed line represents the large a_2 limit. The numerical value for this limit is 8.2 s for the parameters under consideration.

VII. CONCLUSIONS

In this paper we have derived the thermal and spontaneous spin-flip rates for a neutral two-level cold atom that is coupled to the magnetic radiation field of an absorbing dielectric body. The spin-flip rate is given in terms of a dyadic Green tensor, i.e. the expression can be applied to a dielectric body with any geometry. An explicit expression for the total spin-flip rate is given for the 3-layer cylindrical geometry of the experiment described in [3]. We compare our numerical results with the measurements in this experiment and we find that, for the atom-surface distance r as under consideration, the theoretical result predicts longer lifetimes than actually measured in the experiment. The discrepancy corresponds to an overall factor of approximately 1.4. This rather small discrepancy leads to the same conclusion as in [3]: The trapping losses are indeed caused by thermal spin-flips.

We have furthermore illustrated how the lifetime depends on the choice of materials (skin depths) of the current-carrying wire and we have shown that, in some regions of the parameter space, a worse conductor gives a longer lifetime. We have also shown that the lifetime in the perfect conductor limit is basically determined by the blackbody radiation. When the dimensions of the wire

and the atom-surface distance r are varied together, the large r behaviour of the lifetime scales as r^4 , i.e. following the same scaling law as a corresponding plane, thick slab. The small wire limit, on the other hand, is harder to understand. Eventually, our formalism breaks down in this limit. Most likely this breakdown happens far below the micrometer length scale we are considering in this paper. Furthermore, keeping the atom-surface distance fixed and varying the dimensions of the wire, the lifetime scales roughly as the inverse cubed of the radius of the wire provided that the dimensions of wire is scaled sufficiently down.

Acknowledgments

The authors would like to thank M.P.A. Jones for valuable discussions and helpful comments. This work was supported in part by the UK Engineering and Physical Science Research Council and by FASTnet network of the European Union. P.K.R. acknowledges support by the Research Council of Norway. S.S. acknowledges support by the Alexander von Humboldt foundation.

APPENDIX A: THE SCATTERING REFLECTION COEFFICIENTS

The scattering reflection coefficients for a cylindrical geometry can be computed for any number of layers (see e.g. Refs. [10, 12, 13, 14]). In this Appendix we present the explicit expressions for the scattering reflection coefficients corresponding to our 3-layer cylindrical geometry. To find these reflection coefficients we have used the iteration tensor equations in Ref. [10]. These iteration equations are given for arbitrary complex permittivity ε_p and arbitrary complex permeability μ_p . Therefore, reflection coefficients presented in this Appendix yield for arbitrary ε_p and arbitrary μ_p . However, we stress that the whole theory in this paper is *only* applied to non-magnetic media, i.e. $\mu_p = \mu_0$ for all layers p . It is therefore assumed that we put $\mu_p = \mu_0$ in every reflection coefficient when computing the spin-flip rate.

The reflection coefficients are given as follows:

$$R_n^{11}(h) = \frac{(-1)}{d_{n32}} \left[a_{n\mu_3}^{H'_3 J_2} a_{n\varepsilon_3}^{J'_3 J_2} + b_n^{H_3 J_2} b_n^{J_3 J_2} \right] + \left(\frac{2\omega}{\pi a_2} \right)^2 \eta_3^2 \eta_2^2 \varepsilon_3 \frac{T_n^{11}}{N_n}, \quad (\text{A1})$$

$$R_n^{12}(h) = \frac{1}{d_{n32}} \left[a_{n\mu_3}^{H'_3 J_2} b_n^{J_3 J_2} - a_{n\mu_3}^{J'_3 J_2} b_n^{H_3 J_2} \right] + \left(\frac{2\omega}{\pi a_2} \right)^2 \eta_3^2 \eta_2^2 \mu_3 \frac{T_n}{N_n}, \quad (\text{A2})$$

where

$$T_n^{11} = d_{n32} \alpha_n - t_{n21} \beta_n, \quad (\text{A3})$$

$$T_n = d_{n32} \gamma_n - t_{n21} \delta_n, \quad (\text{A4})$$

and

$$N_n = (d_{n32})^2 \left[d_{n32} d_{n21} + t_{n21} t_{n32} - (a_{11} b_{11} - 2 \frac{\varepsilon_2}{\mu_2} a_{12} b_{12} + a_{22} b_{22}) \right]. \quad (\text{A5})$$

The reflection coefficients $R_n^{21}(h)$ and $R_n^{22}(h)$ can be obtained from $R_n^{12}(h)$ and $R_n^{11}(h)$, respectively, by replacing $\mu_p \leftrightarrow -\varepsilon_p$. Moreover, we have

$$\alpha_n = -(a_{n\mu_3}^{H'_3 J_2})^2 \varepsilon_2 b_{11} + (b_n^{H_3 J_2})^2 \mu_2 b_{22} - 2 \varepsilon_2 b_{12} a_{n\mu_3}^{H'_3 J_2} b_n^{H_3 J_2}, \quad (\text{A6})$$

$$\beta_n = -(a_{n\mu_3}^{H'_3 J_2})^2 \varepsilon_2 a_{22} + (b_n^{H_3 J_2})^2 \mu_2 a_{11} + 2 \varepsilon_2 a_{12} a_{n\mu_3}^{H'_3 J_2} b_n^{H_3 J_2}, \quad (\text{A7})$$

$$\gamma_n = -a_{n\mu_3}^{H'_3 J_2} b_n^{H'_3 J_2} \varepsilon_3 b_{11} - a_{n\varepsilon_3}^{H'_3 J_2} b_n^{H_3 J_2} \mu_2 b_{22} + \varepsilon_2 b_{12} [a_{n\mu_3}^{H'_3 J_2} a_{n\varepsilon_3}^{H'_3 J_2} - (b_n^{H_3 J_2})^2], \quad (\text{A8})$$

$$\delta_n = -a_{n\mu_3}^{H'_3 J_2} b_n^{H_3 J_2} a_{22} - a_{n\varepsilon_3}^{H'_3 J_2} b_n^{H_3 J_2} \mu_2 a_{11} - \varepsilon_2 a_{12} [a_{n\mu_3}^{H'_3 J_2} a_{n\varepsilon_3}^{H'_3 J_2} - (b_n^{H_3 J_2})^2], \quad (\text{A9})$$

and

$$a_{11} = a_{n\mu_3}^{H'_3 J_2} a_{n\varepsilon_3}^{H'_3 H_2} + b_n^{H_3 J_2} b_n^{H_3 H_2}, \quad (\text{A10})$$

$$a_{12} = a_{n\mu_3}^{H'_3 J_2} b_n^{H_3 H_2} - a_{n\mu_3}^{H'_3 H_2} b_n^{H_3 J_2} = -\frac{2\omega}{\pi a_2} \eta_3^2 \frac{h n}{a_2} \mu_2 (H_{n3})^2 (k_2^2 - k_3^2), \quad (\text{A11})$$

$$b_{11} = a_{n\mu_2}^{H'_2 J_1} a_{n\varepsilon_2}^{J'_2 J_1} + b_n^{H_2 J_1} b_n^{J_2 J_1}, \quad (\text{A12})$$

$$b_{12} = a_{n\mu_2}^{H'_2 J_1} b_n^{J_2 J_1} - a_{n\mu_2}^{J'_2 J_1} b_n^{H_2 J_1} = -\frac{2\omega}{\pi a_1} \eta_1^2 \frac{h n}{a_1} \mu_2 (J_{n1})^2 (k_1^2 - k_2^2). \quad (\text{A13})$$

The function a_{21} , a_{22} , and b_{21} , b_{22} are obtained from a_{12} , a_{11} , and b_{12} , b_{11} , respectively, by replacing $\mu_p \leftrightarrow \varepsilon_p$. In the last step in Eqs. (A11) and (A13) we have used the Wronskian determinant between Bessel and Hankel functions. Finally, we have

$$t_{n21} = a_{n\mu_2}^{J'_2 J_1} a_{n\varepsilon_2}^{J'_2 J_1} + (b_n^{J_2 J_1})^2, \quad (\text{A14})$$

$$t_{n32} = a_{n\varepsilon_3}^{H'_3 H_2} a_{n\mu_3}^{H'_3 H_2} + (b_n^{H_3 H_2})^2, \quad (\text{A15})$$

$$d_{n21} = a_{n\mu_2}^{H'_2 J_1} a_{n\varepsilon_2}^{H'_2 J_1} + (b_n^{H_2 J_1})^2, \quad (\text{A16})$$

$$d_{n32} = a_{n\mu_3}^{H'_3 J_2} a_{n\varepsilon_3}^{H'_3 J_2} + (b_n^{H_3 J_2})^2, \quad (\text{A17})$$

and

$$a_{n\mu_2}^{H'_2 J_1} = i\omega \eta_2 \eta_1 (\mu_2 \eta_1 H_{n2}^{J_1} J_{n1} - \mu_1 \eta_2 H_{n2}^{J_1} J_{n1}) \quad (\text{A18})$$

$$a_{n\mu_2}^{J'_2 J_1} = i\omega \eta_2 \eta_1 (\mu_2 \eta_1 J_{n2}^{J_1} J_{n1} - \mu_1 \eta_2 J_{n2}^{J_1} J_{n1}), \quad (\text{A19})$$

$$a_{n\varepsilon_2}^{H'_2 J_1} = i\omega \eta_2 \eta_1 (\varepsilon_2 \eta_1 H_{n2}^{J_1} J_{n1} - \varepsilon_1 \eta_2 H_{n2}^{J_1} J_{n1}) \quad (\text{A20})$$

$$a_{n\varepsilon_2}^{J'_2 J_1} = i\omega \eta_2 \eta_1 (\varepsilon_2 \eta_1 J_{n2}^{J_1} J_{n1} - \varepsilon_1 \eta_2 J_{n2}^{J_1} J_{n1}), \quad (\text{A21})$$

$$b_n^{H_2 J_1} = \frac{h n}{a_1} H_{n2}^{J_1} J_{n1} (k_1^2 - k_2^2). \quad (\text{A22})$$

Whenever the combination Z_2 and Z_1 is involved in the superscript, the radius a_1 is implicit in the cylindrical functions. For example, in Eqs. (A18)–(A22) we have

$$Z_{n1} \equiv Z_n(\eta_1 a_1), Z_{n2} \equiv Z_n(\eta_2 a_1), \quad (\text{A23})$$

$$Z'_{n1} \equiv \frac{dZ_n(\eta_1 a_1)}{d(\eta_1 a_1)}, \quad Z'_{n2} \equiv \frac{dZ_n(\eta_2 a_1)}{d(\eta_2 a_1)}. \quad (\text{A24})$$

The functions $a_{n\mu_3}^{H'_3 J_2}$, $a_{n\mu_3}^{J'_3 J_2}$, $a_{n\varepsilon_3}^{H'_3 J_2}$, $a_{n\varepsilon_3}^{H'_3 H_2}$, $a_{n\varepsilon_3}^{J'_3 J_2}$, $b_n^{H_3 J_2}$,

and $b_n^{H_3 H_2}$ are defined analogously, where we understand that the radius a_2 is implicit in all those functions. Of course, for the special case $\mu_p = 1$ for all layers p , these reflection coefficients simplify.

Note that the scattering coefficients $R_n^{11}(h)$ as well as $R_n^{22}(h)$ are dimensionless. However, the coefficients $R_n^{12}(h)$ and $R_n^{21}(h)$ are not, but the particular combinations $R_n^{12}(h)(-\omega\varepsilon_3/k_3) = R_n^{21}(h)(\omega\mu_3/k_3)$ are.

- [1] E.A. Hinds and I.A. Hughes, *J. Phys. D: Appl. Phys.* **32**, R119 (1999); R. Folman, P. Krüger, J. Schmiedmayer, J. Denschlag, and C. Henkel, *Adv. At. Mol. Opt. Phys.* **48**, 263 (2002).
- [2] J.B. Johnson, *Phys. Rev.* **32**, 97 (1928); H. Nyquist, *Phys. Rev.* **32**, 110 (1928).
- [3] M.P.A. Jones, C.J. Vale, D. Sahagun, B.V. Hall, and E.A. Hinds, *Phys. Rev. Lett.* **91**, 080401 (2003).
- [4] D.M. Harber, J.M. McGuirk, J.M. Obrecht, and E.A. Cornell, *J. Low. Temp. Phys.* **133**, 229–238 (2003).
- [5] C. Henkel, S. Pötting and M. Wilkens, *Appl. Phys. B* **69**, 379 (1999); C. Henkel and M. Wilkens, *Europhys. Lett.* **47**, 414 (1999).
- [6] L. Knöll, S. Scheel, and D.-G. Welsch, *QED in dispersing and absorbing media*, in *Coherence and Statistics of Photons and Atoms*, ed. J. Peřina (Wiley, New York, 2001); S. Scheel, L. Knöll and D.-G. Welsch, *Phys. Rev. A* **60**, 1590 (1999); S. Scheel, L. Knöll and D.-G. Welsch, *Phys. Rev. A* **60**, 4094 (1999); T.D. Ho, L. Knöll and D.-G. Welsch, *Phys. Rev. A* **62**, 053804 (2000).
- [7] G.S. Agarwal, *Phys. Rev. A* **11**, 230 (1975); J.M. Wylie and J.E. Sipe, *Phys. Rev. A* **30**, 1185 (1984).
- [8] L.D. Landau and E.M. Lifshitz, *Electrodynamics of continuous media*, (Pergamon Press, Oxford, 1960).
- [9] L. Onsager, *Phys. Rev.* **37**, 405 (1931); **38**, 2265 (1931);
- [10] W.C. Chew, *Waves and Fields in Inhomogeneous Media*, IEEE Press Series on Electromagnetic Waves (1990).
- [11] J.D. Jackson, *Classical Electrodynamics*, 2nd edn., (Wiley, New York, 1975).
- [12] C.-T. Tai, *Dyadic Green Functions in Electromagnetic Theory*, IEEE Press Series on Electromagnetic Waves (1993).
- [13] Z. Xiang and Y. Lu, *IEEE Trans. Microwave Theory Tech.* **44**, 614 (1996).
As pointed out in Ref. [14], this paper contains some critical mistakes. The relation between the scattering coefficients and the Green tensor in this reference is not consistent.
- [14] L.-W. Li, M.-S. Leong, T.-S. Yeo, and P.-S. Kooi, *J. of Electromagnetic Waves and Appl.* **14**, 961 (2001).
- [15] In Ref. [3], the angular factor is erroneously given by 1/10.